

28 GHz Channel Measurements in the COSMOS Testbed Deployment Area

Tingjun Chen¹, Manav Kohli¹, Tianyi Dai¹, Angel Daniel Estigarribia¹,
Dmitry Chizhik², Jinfeng Du², Rodolfo Feick³, Reinaldo A. Valenzuela², Gil Zussman¹
¹Electrical Engineering, Columbia University, ²Nokia Bell Labs, ³Universidad Técnica Federico Santa María
{tingjun@ee., manav.kohli@, td2593@, ade2119@, gil@ee.}columbia.edu,
{dmitry.chizhik, jinfeng.du, reinaldo.valenzuela}@nokia-bell-labs.com, rodolfo.feick@usm.cl

ABSTRACT

Next generation wireless and mobile networks will utilize millimeter-wave (mmWave) communication to achieve significantly increased data rates. However, since mmWave radio signals experience high path loss, the operation of mmWave networks will require accurate channel models designed for specific deployment sites. In this paper, we focus on the deployment area of the PAWR COSMOS testbed [1, 2] in New York City and report extensive 28 GHz channel measurements. These include over 24 million power measurements collected from over 1,500 links on 13 sidewalks in 3 different sites and in different settings during March–June, 2019. Using these measurements, we study the effects of the setup and environments (e.g., transmitter height and seasonal effects). We then discuss the obtained path gain values and their fitted lines, and the resulting effective azimuth beamforming gain. Based on these results, we also study the link SNR values that can be supported on individual sidewalks and the corresponding theoretically achievable data rates. We believe that the results can inform the COSMOS testbed deployment process and provide a benchmark for other deployment efforts in dense urban areas.

CCS CONCEPTS

• **General and reference** → **Measurement**; • **Networks** → *Network measurement*; *Wireless access networks*; *Physical links*.

KEYWORDS

28 GHz; millimeter-wave; channel measurements; COSMOS testbed

ACM Reference Format:

Tingjun Chen, Manav Kohli, Tianyi Dai, Angel Daniel Estigarribia, Dmitry Chizhik, Jinfeng Du, Rodolfo Feick, Reinaldo A. Valenzuela, Gil Zussman. 2019. 28 GHz Channel Measurements in the COSMOS Testbed Deployment Area. In *3rd ACM Workshop on Millimeter-wave Networks and Sensing Systems (mmNets'19)*, October 25, 2019, Los Cabos, Mexico. ACM, New York, NY, USA, 6 pages. <https://doi.org/10.1145/3349624.3356770>

Permission to make digital or hard copies of all or part of this work for personal or classroom use is granted without fee provided that copies are not made or distributed for profit or commercial advantage and that copies bear this notice and the full citation on the first page. Copyrights for components of this work owned by others than the author(s) must be honored. Abstracting with credit is permitted. To copy otherwise, or republish, to post on servers or to redistribute to lists, requires prior specific permission and/or a fee. Request permissions from permissions@acm.org.

mmNets'19, October 25, 2019, Los Cabos, Mexico

© 2019 Copyright held by the owner/author(s). Publication rights licensed to ACM.
ACM ISBN 978-1-4503-6932-9/19/10...\$15.00
<https://doi.org/10.1145/3349624.3356770>

1 INTRODUCTION

Millimeter-wave (mmWave) communication, which uses the widely available spectrum to achieve significantly increased data rates, is a key technology for next generation wireless networks [3, 4]. It is also beneficial to higher layer protocols [5] and has the potential to support a broad class of new applications such as high-resolution localization and sensing [6], and augmented/virtual reality [7].

To support the design and deployment of mmWave networks, it is important to understand the fundamental propagation properties of mmWave signals and the corresponding effects on the system-level performance in different network scenarios. Radio signals at mmWave frequencies experience significantly lower path gain (or higher path loss) and are more vulnerable to environmental changes (e.g., object blockage and movement) compared to signals at lower frequencies (e.g., sub-6 GHz). Therefore, directional antennas [8–10] and beamforming using phased arrays [10–13] have been applied to mitigate the low path gain. Moreover, the operation of mmWave networks will require accurate channel models designed for specific types of deployment site.

In this paper, we focus on the deployment area of the PAWR COSMOS testbed [1, 2] – a city-scale programmable testbed for experimentation with advanced wireless that is being deployed in New York City (see Fig. 1). We report extensive 28 GHz channel measurements in this area, which is a representative urban street canyon environment with both line-of-sight (LOS) and non-light-of-sight (NLOS) links. In particular, we consider 3 sites that emulate different deployment scenarios of a mmWave base station (BS): (i) a 15 m-high balcony at a 4-way street intersection (referred to as “Intersection Balcony [Int]”), (ii) a 6 m-high bridge over-crossing an avenue (referred to as “Bridge [Bri]”), and (iii) a 15 m-high balcony facing a park (referred to as “Open Balcony [Bal]”).

Our measurement campaign includes over 1,500 link measurements (with over 24 million power measurements) collected along 13 sidewalks adjacent to the 3 considered measurement sites. The channel measurements are collected using a portable 28 GHz narrowband channel sounder with a transmitter (Tx) and a rotating receiver (Rx). We first consider the effects of the measurement setup and the environment. In particular, we consider swapped Tx and Rx locations, raised Tx heights, and seasonal effects. We conducted various measurements and experimentally observed that these effects are minimal on the considered sidewalks. For example, the path gain fitted lines for Tx heights of 1.5 m and 3 m differ by only less than 3 dB over link distances of 40–500 m.

We then present and discuss the measurement results on the path gain values and their fitted lines, and the effective azimuth

beamforming gain. In particular, we compare between different sidewalk groups and between individual sidewalks in Int. The results show that, even in the NLOS scenario, the measured path gain values are on average 5–10 dB higher than that provided by the 3GPP 38.901 urban canyon NLOS model [14]. Moreover, the median azimuth beamforming gain is within 1.7 dB and 2.9 dB of their nominal values for sidewalks with LOS and NLOS, respectively.

Moreover, based on the measurement results, we consider the link SNR values that can be achieved on individual sidewalks. In particular, link SNR values of at least 15 dB can be achieved on all sidewalks up to 194 m link distance. This distance increases to 300 m on sidewalks with higher path gain values. We also discuss the theoretically achievable data rates in the considered area. We believe that our measurement results can provide insight into the deployment of the 28 GHz phased array antenna modules (PAAMs) (developed by IBM and Ericsson [11]), in the COSMOS testbed. The results can also serve as the benchmark for the experimentation with these modules once deployed.

2 RELATED WORK

Various channel measurement campaigns have been conducted for different mmWave frequencies (e.g., 28/38/73 GHz) in urban [3, 9, 15, 16] and suburban [3, 8, 17, 18] environments. Both directional horn antennas on mechanical steering platforms [8–10] and phased arrays applying beam steering [10–13] were considered. With the support of wideband channel sounders, these campaigns can provide measurements of not only the path gain, but also other metrics such as the power delay profile. However, most of these campaigns consider limited number of measurement links (usually at the order of 10s) with different Tx and Rx locations. Recent work also demonstrates link-level channel measurements using commercial 802.11ad devices [19, 20].

Unlike some of the previous work, we use a narrowband channel sounder that, on the other hand, can uniquely support (i) fast recording of received signal on the entire 360° azimuth plane (and thereby the effective azimuth beamforming gain), and (ii) easy and continuous measurements on relatively long streets with small measurement step sizes (see Section 3). Hence, our measurement campaign focuses on accurately characterizing the mmWave channel *along individual streets* with small link distance step sizes. This results in extensive amount of collected measurement data.

3 MEASUREMENTS: EQUIPMENT, ENVIRONMENTS, AND DATASET

3.1 Measurement Equipment

To maximize data collection speed and link budget, we use a 28 GHz portable narrowband channel sounder with a transmitter (Tx) and a rotating receiver (Rx) (more details can be found in [21]). In particular, the Tx is equipped with an omni-directional antenna (with 0 dBi gain) and emits a 28 GHz continuous-wave tone at +22 dBm power. The Rx is equipped with a horn antenna with 24 dBi gain and 10° half-power beamwidth, which is connected to a low-noise amplifier, a mixer, and a USB power meter with a bandwidth of 20 kHz and an effective noise figure of 5 dB. The Rx is mounted on a rotating platform, which allows for a full 360° angular scan in the azimuth plane every 500 ms (at rotational speed of 120 rpm). Using

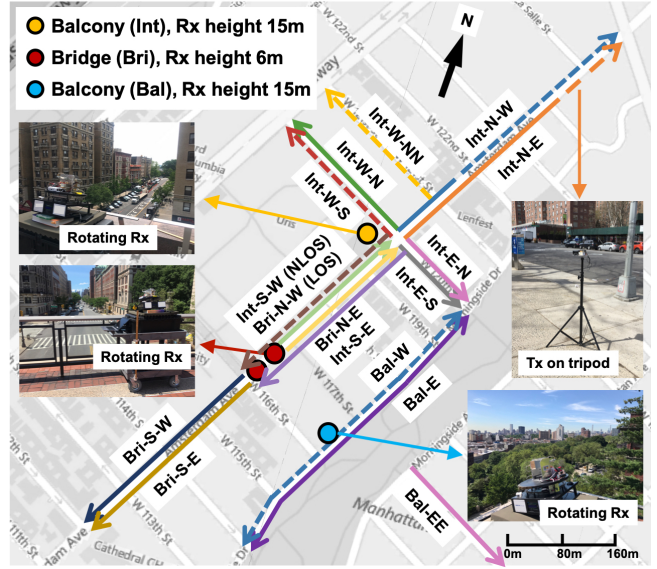


Figure 1: Locations and example street views of the three measurement sites in the COSMOS testbed deployment area. The receiver (Rx) is placed at a fixed location in each site (marked by a circle), and the transmitter (Tx) is moved along the measurement sidewalks (marked by lines). Solid and dashed lines correspond to sidewalks (or part of the sidewalks) where the Tx and Rx are in line-of-sight (LOS) and non-line-of-sight (NLOS), respectively.

an onboard Raspberry Pi, the Rx records power samples at a rate of 740 samples per second. Both the Tx and Rx have free running local oscillators (LOs) with a frequency accuracy of at least 10^{-7} , and are powered by batteries to support portable measurements.

The channel sounder system is calibrated in the lab and in an anechoic chamber to ensure an absolute power accuracy of 0.15 dB. The full dynamic range of the Rx is 50 dB (from the Rx noise floor to its 1 dB compression point). The Rx also includes two switchable power amplifiers which can further extend the dynamic range to 75 dB (when both power amplifiers are switched on). Together with the use of removable attenuators at the Tx, the channel sounder supports a range of measurable path gain with at least 10 dB SNR from -62 dB to -137 dB. This corresponds to 1 m range in free space to 200 m range with 30 dB excess loss. The measurable path gain extends to -161 dB with the 24 dBi Rx horn antenna.

3.2 Measurement Environment

We perform extensive 28 GHz channel measurements in the deployment area of the PAWR COSMOS testbed [1, 2], which is currently being deployed in West Harlem, New York City. Fig. 1 shows the map of the measurement area and example street views in the measurement locations. The considered area is a representative *urban street canyon* environment containing mostly concrete and brick buildings with heights of 10–60 m (3–16 stories). The vegetation in the measurement area consists of sparse thin trees separated equally on both sides on the city streets, representative of North-eastern U.S. cities. As shown in the map, the area is bordered by two parks (Riverside Park and Morningside Park).

We consider 3 measurement sites representing different deployment scenarios of a mmWave small cell BS (see Fig. 1):

- Intersection Balcony (Int): the 4th floor balcony (with a height of 15 m) in the SW corner of the intersection of Amsterdam Avenue

Table 1: Summary of (i) the measurement campaign setup on 13 sidewalks in 3 sites (Intersection Balcony [Int], Bridge [Bri], and Open Balcony [Bal]), as shown in Fig. 1, and 4 sidewalk groups (Int-LOS, Int-NLOS, Bri, and Bal), (ii) the slope (n), intercept (b), and root mean square (RMS, σ) values for the path gain fitted lines, and (iii) the median and 10th-percentile azimuth gain values.

Sidewalk Name	Sidewalk Color	Sidewalk Group	Sidewalk Length (m)	Meas. Step Size (m)	# of Meas. Links	Slope (n)	Intercept (b [dB])	RMS (σ [dB])	Median Azi. Gain (dBi)	10 th -perc. Azi. Gain (dBi)
Int-N-E	Orange	Int-LOS	507	3/6 (near/far)	101	-3.5	-36.8	4.3	14.1	12.3
Int-W-N	Dark Green	Int-LOS	256	3	79	-2.6	-52.2	4.4	14.2	13.2
Int-S-E	Light Purple	Int-LOS	317	3	93	-3.4	-35.5	4.6	14.2	13.4
Int-E-N	Pink	Int-LOS	146	1.5	85	-2.3	-60.3	4.5	14.2	13.1
Int-E-S	Gray	Int-LOS	146	1.5	88	-2.8	-49.5	3.2	14.1	12.4
Int-N-W	Light Blue	Int-NLOS	509	3	139	-3.6	-36.0	3.6	13.1	11.8
Int-W-S	Red	Int-NLOS	256	3	69	-3.1	-47.5	3.1	11.6	10.4
Int-S-W	Brown	Int-NLOS	317	3	100	-3.6	-39.2	3.4	12.9	11.2
Bri-N-E	Yellow	Bri	219	3	65	-2.3	-60.0	3.9	12.6	11.3
Bri-N-W	Light Green	Bri	219	3	70	-2.6	-52.5	4.3	13.4	11.7
Bri-S-E	Dark Yellow	Bri	280	3/6 (near/far)	84	-2.5	-55.7	5.5	12.8	11.6
Bri-S-W	Dark Blue	Bri	280	3/6 (near/far)	87	-2.2	-59.8	4.0	13.2	11.4
Bal-E-E	Purple	Bal	488	3	156	-3.4	-47.2	5.8	13.9	12.8

and West 120th street.¹ This location emulates the scenario where the BS is deployed on building roof/side in an urban street canyon;

- Bridge (**Bri**): the bridge (with a height of 6 m) crossing above Amsterdam Avenue between West 116th and 117th streets. This emulates the scenario where the BS is deployed on a lightpole in the middle of a two-way avenue;
- Open Balcony (**Bal**): the balcony of the Faculty House (with a height of 15 m) facing Morningside Park, where the neighboring buildings are 4–16 stories high. This emulates the scenario where the BS is deployed on the building roof and/or building side facing an open-space area.²

The channel measurements are collected on 8/4/1 sidewalks³ in sites Int/Bri/Bal, respectively. In Fig. 1, each sidewalk is represented by a line with an arrow pointing from the corresponding Rx in the site. On most sidewalks, direct LOS (*solid* lines in Fig. 1) exists between the Tx and Rx despite possible blockages such as foliage and trees, street signs, lightpoles, etc. Although LOS with these types of blockage is typically considered as NLOS, we categorize these sidewalks as LOS to distinguish from the “true” NLOS case caused by the street canyon environment (e.g., strong blockage by concrete buildings) as illustrated by the *dashed* lines in Fig. 1.

We categorize three sidewalks in group Int-NLOS where: (i) Tx on Int-W-S (red line) and Int-S-W (brown line) are right underneath the Rx with no direct LOS, and (ii) Tx on Int-N-W (light blue line) is blocked from the Rx by the buildings on the same side of the street. By exploring the angle-of-arrival (AoA) of the angular spectrum at the Rx, it can be observed that most of the received signal power comes from diffraction and/or reflections off building edges/walls on sidewalks in the Int-NLOS group.⁴

For each site, the rotating Rx with a 10° horn antenna is used to emulate the BS with better angular resolution in order to capture signals arriving from all azimuth directions. The Tx with an omnidirectional antenna, emulating a user equipment (UE), is placed on a tripod and is moved along the sidewalks to obtain link measurements as a function of the link distance. On most sidewalks, the Tx

is moved away from the Rx at a step size of 3 m in short distances, and at a step size of 6 m in long distances (i.e., $d > 250$ m).⁵ Two exceptional sidewalks are Int-E-N/S, where the Tx is moved away from the Rx at a smaller step size of 1.5 m to ensure enough number of measurement links on shorter sidewalks.

For a given pair of Tx and Rx locations, we record one link measurement which lasts for 20 seconds and consists of 40 full 360° azimuth scans. The link distance of each measurement is calculated using the 3D geometric coordinates obtained from Google Earth with terrain characteristics (e.g., the elevation/slope of each sidewalk) taken into account. For example, sidewalks Int-N-W and Int-N-E are going downhill from south to the north, and the resulting relative height between the Rx and Tx is 15/41 m at the nearest/furthest (southernmost/northernmost) location, respectively.

Table 1 summarizes our measurement campaign on the 13 sidewalks during March–June, 2019, where the sidewalk color corresponds to the colored lines in Fig. 1. Over 1,500 link measurements were collected. For each link measurement, over 15,000 power samples were collected during 20 seconds as a function of both time and azimuth angle, from which the path gain and effective azimuth gain can be computed (see Section 3.3). Overall, a total number of over 24 million power measurements were collected.

3.3 Path Gain and Azimuth Gain

As described above, the rotating Rx with a horn antenna can record the received signal power as a function of both time and the azimuth angle. Following the methodology described in [21], we now briefly describe the calculation for two considered performance metrics: (i) path gain, PG, and (ii) effective azimuth gain, G_{az} , which quantifies the effects of scattering environments on the signal angular spread, and thus the effective beamforming gain.

Denote by $P(d, \phi)$ the instantaneous received power measurement at link distance of d (m) in the azimuth direction of ϕ . It is shown in [21] that the average power for each link measurement with distance d , denoted by $\bar{P}(d)$ (obtained by averaging $P(d, \phi)$ over the azimuth angle, ϕ , using a directional antenna) equals to that measured using an omnidirectional antenna, i.e.,

$$\bar{P}_{\text{horn}}(d) = \frac{1}{2\pi} \cdot \int_{\phi=0}^{2\pi} P(d, \phi) d\phi = \bar{P}_{\text{omni}}(d). \quad (1)$$

¹The COSMOS pilot nodes are located at this intersection.

²Note that this deployment scenario is common throughout Manhattan such as in streets adjacent to Riverside Park, Central Park, and St. Nicholas Park (where the COSMOS nodes in City College of New York are expected to be deployed).

³We differentiate two sidewalks of the same street with different labels, e.g., Int-N-E and Int-N-W correspond to the East and West sides of Int-N (i.e., Amsterdam Avenue between West 120th and 125th streets), respectively.

⁴Further explorations and studies on the effects of diffraction and reflections in urban street canyon environments is a subject of our future research.

⁵In the measurement area, a street block is approximately 80 m long, and a street tile size is 1.5 m × 1.5 m.

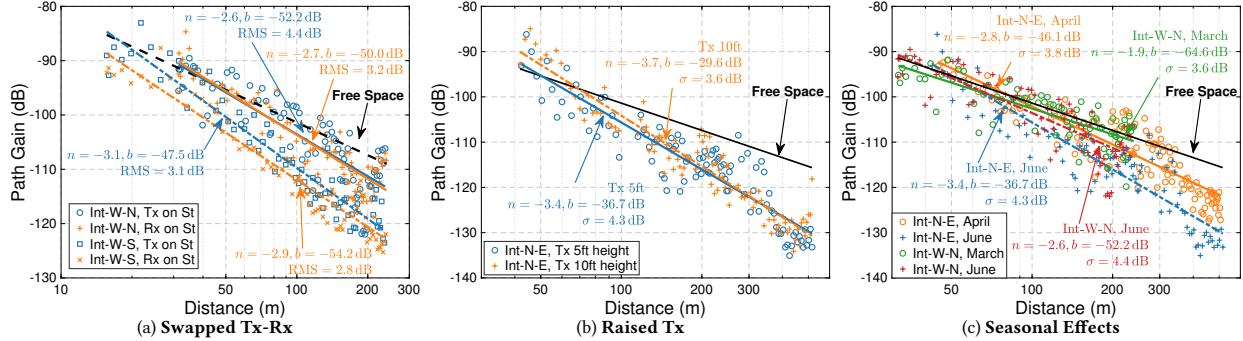


Figure 2: Measured path gain values and their fitted lines for understanding the effects of the measurement setup and environments. Considered effects include: (a) Swapped Tx-Rx: Relative locations between the Tx and Rx, (b) Raised Tx: Height of the Tx, and (c) Seasonal Effects: Vegetation depth and foliage on the sidewalks.

The path gain as a function of the link distance, $PG(d)$, is then computed as the received signal power level when removing the Tx power, P_{Tx} , and the antenna elevation gain, G_{el} (recall that the Rx is rotating on the azimuth plane), i.e.,

$$PG(d) = \bar{P}_{\text{horn}}(d) / (P_{Tx} \cdot G_{el}), \quad (2)$$

where G_{el} is the Rx antenna elevation gain measured in an anechoic chamber. Accordingly, the effective azimuth beamforming gain is defined as the peak-to-average ratio of the receive power measurements, which is given by

$$G_{\text{az}}(d) = \max_{\phi} \{P(d, \phi)\} / \bar{P}_{\text{horn}}(d). \quad (3)$$

The measured path gain values are linearly curve-fitted by

$$PG(d) = 10n \cdot \log_{10} d + b + \mathcal{N}(0, \sigma) \text{ (dB)}, \quad (4)$$

where n , b , and σ are the slope, intercept, and root mean square (RMS) of the fitted line. For brevity, we refer to these parameters of a fitted line by their variables throughout the paper. The obtained values of n , b , and σ for the sidewalks are summarized in Table 1 and are discussed in Section 4. Note that the *Friis free space* path gain line is with $n = -2$, $b = -61.4$ dB, and $\sigma = 0$ dB.

4 MEASUREMENT RESULTS

We now present and discuss the measurement results of the path gain values and the effective azimuth beamforming gain in the 3 measurement sites (see Fig. 1 and Table 1).

4.1 Effects of Setup and Environments

Conducting ideal and controllable channel measurements in an urban street canyon environment is challenging, due to various factors such as the measurement setup and environments. In order to better understand the possible effects of these factors on the results, we first conduct three basic sets of measurements to study the following effects: (i) **Swapped Tx-Rx**: relative locations between the Tx and Rx, (ii) **Raised Tx**: height of the Tx, and (iii) **Seasonal Effects**: vegetation depth and foliage on the sidewalks.

Swapped Tx-Rx. Recall that we use the Rx to emulate the BS due to its capability to capture received power across the full 360° azimuth plane. Ideally, swapping the placement of the omni-directional Tx antenna and a rotating directional Rx antenna is expected to result in the same average power with proper compensation of the vertical beam pattern effects. We first conduct measurements to verify this and to understand the sensitivity to swapped Tx and Rx locations.⁶

⁶Channel reciprocity is valid when swapping Tx and Rx while leaving antennas in place. Here, the Tx and Rx antennas are also swapped together with the platform.

In particular, we consider sidewalks Int-W-N and Int-W-S with the Tx (resp. the rotating Rx) placed on the intersection balcony and the street (resp. the street and intersection balcony).⁷

Fig. 2(a) shows the measured path gain values and their fitted lines for the four measurements on two sidewalks. It can be seen that the link measurements on the same street but with swapped Tx and Rx locations are similar, where the differences in n (slope) and b (intercept) of the fitted lines are 0.1/0.2 and 2.2/6.7 dB for Int-W-N/Int-W-S, respectively. Due to the more complex environmental effects in the NLOS channels, the measured path gains on Int-W-S are on average lower than that on Int-W-N. These results show that swapping the Tx and Rx locations has only minimal effects on the path gain. Therefore, throughout the rest of the measurements, we use the rotating Rx with better angular resolution to emulate the BS with heights of 6–15 m (see Section 3.2).

Raised Tx. We evaluate the effects of the Tx height by placing the Tx on a tripod at 1.5/3.0 m and measuring the path gains on sidewalk Int-N-E.⁸ Fig. 2(b) shows the measured path gains, whose fitted lines for both Tx heights differ by only 2.5 dB and 0.8 dB at the near ($d = 50$ m) and far ($d = 500$ m) ends, respectively. Although at different heights, the Tx experiences slightly different channel characteristics (e.g., blockage by trees), the measured path gains are similar, with less than 3 dB difference between the fitted lines over link distances of 40–500 m.

Seasonal Effects. Finally, we evaluate the seasonal effects during the period of March–June, 2019. In particular, we conducted measurements on Int-N-E and Int-W-N in two different months (all in sunny days) where the foliage and the depth of the tree leaves vary between early spring (no leaves) and summer (full leaves).⁹ Fig. 2(c) shows the measured path gains and their fitted lines. The results show that the differences between months are minimal for d up to 250 m. Note that for $d > 250$ m on Int-N-E, the path gain values measured in the summer (June) drop by around 10 dB compared to that measured in early spring (April). This could possibly stem from the fact that the aggregated effects of the foliage along the street is more significant in the summer. We plan to conduct more comprehensive measurements in the fall/winter to further investigate the effects of foliage on the path gains.

Overall, we believe that the measurements are good representative of the three effects on the corresponding streets, and hence can

⁷In Table 1, the rows of Int-W-N and Int-W-S are with Rx on the intersection balcony.

⁸In Table 1, the row of Int-N-E is with Tx at 1.5 m height.

⁹In Table 1, the rows of Int-N-E and Int-W-N correspond to their measurements conducted in June 2019.

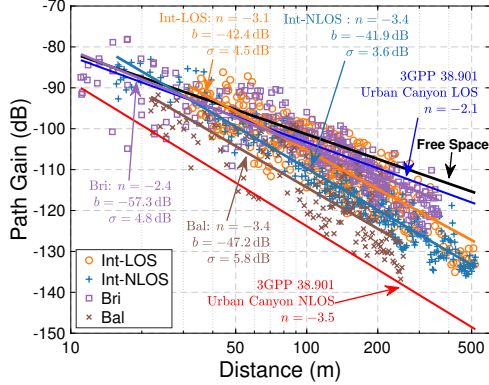


Figure 3: Measured path gain values and the corresponding fitted lines for different sidewalk groups (Int-LOS, Int-NLOS, Bri, and Bal).

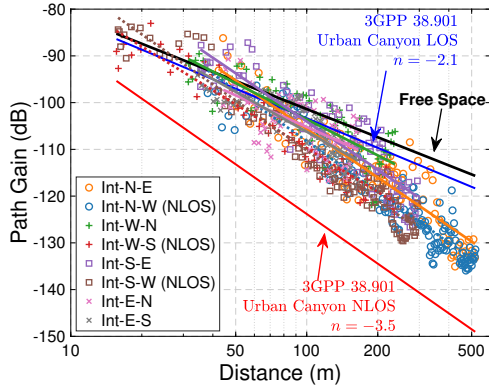


Figure 4: Measured path gain values and the corresponding fitted lines for individual sidewalks in the Intersection Balcony (Int).

provide insight into these effects on other sidewalks in the same area. Yet, we plan to conduct more measurements in the future for further empirical validation. We also plan to study and evaluate other effects including traffic loads and weather, etc.

4.2 Path Gain

We now study different deployment scenarios where the rotating Rx is placed in sites Int/Bri/Bal. These cases correspond to different mmWave BS deployment scenarios as described in Section 3.2.

As shown in Table 1, the sidewalks are categorized into four groups (see also Fig. 1). Fig. 3 shows the measured path gains for each group (in markers) and their fitted lines using the 1,216 link measurements collected. The results show that Int-LOS and Bri have comparable path gains since similar effects of the urban street canyon environment apply in both cases. However, these effects are less significant for Int-NLOS and Bal, where lower measured path gains are observed. We conjecture that this is because of the reduced Rx power that could have been reflected from building sides/walls. Moreover, most path gains fall between the 3GPP 38.901 urban street canyon LOS and NLOS models [14]. Specifically, the values of n , b , and σ for groups Int-LOS/Int-NLOS/Bri/Bal are $-3.1/-3.4/-2.4/-3.4$, $-42.4/-41.9/-57.3/-47.2$ dB, and $4.5/3.6/4.8/5.8$ dB, respectively.

We also consider individual sidewalks in Int and Fig. 4 plots the measured path gain values and their fitted lines. The corresponding parameters for the fitted lines are summarized in Table 1. It can be seen that the measured path gain values are mostly 10 dB higher than the 3GPP 38.901 urban canyon NLOS model, and over 5 dB

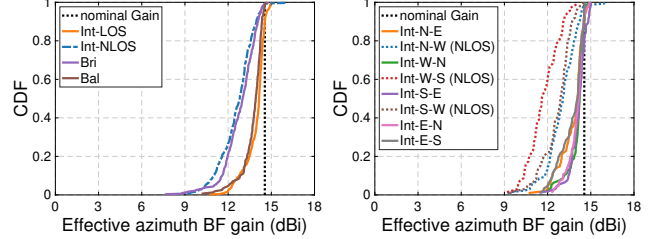


Figure 5: CDFs of the effective azimuth beamforming gain for the sidewalk groups (left) and for individual sidewalks in Intersection Balcony (Int) (right).

lower than the 3GPP 38.901 urban canyon LOS model for distances beyond 100 m.

4.3 Effective Azimuth Beamforming Gain

As mentioned in Section 3.3, the effective azimuth gain characterizes the corresponding beamforming gain under the effects of scattering environments on the angular spread of the signal. Fig. 5 plots the CDFs of the effective azimuth beamforming gain of groups Int-LOS/Int-NLOS/Bri/Bal (left) and of individual sidewalks at Int (right). In particular, the median azimuth gains for Int-LOS/Int-NLOS/Bri/Bal are 14.2/12.8/13.0/13.9 dB, respectively, which are very similar across different sites. Both the median and 10th-percentile azimuth gains for individual streets in Int are summarized in Table 1. It can be seen that: (i) the 10th-percentile azimuth gain is at most 1.8 dB lower than the median azimuth gain across all sidewalks, and (ii) the beamforming gain degradation is more significant on NLOS sidewalks (e.g., the median azimuth beamforming gain is always within 1.7/2.9 dB of the nominal value for sidewalks with LOS/NLOS, respectively).

5 SNR COVERAGE

Empirical path gain models based on extensive measurements (such as those discussed in Sections 3 and 4) will allow performance evaluation of mmWave networks in various settings. In this section, we consider link SNR values that can be achieved in the COSMOS testbed deployment area. These values can provide insight into characterizing the coverage at 28 GHz and the achievable data rates.

We assume the following parameters. The BS has a constant Tx power of $P_{Tx} = +28$ dBm and a maximum Tx gain of 23 dBi.¹⁰ For each sidewalk, the effective Tx gain, denoted by G_{Tx} , is obtained by subtracting the median azimuth gain degradation indicated in Table 1 from the maximum Tx gain. The UE is assumed to have a nominal Rx gain of $G_{Rx} = 11.0$ dBi and a noise figure of 10 dB. We consider signal bandwidth of 800 MHz. The resulting Rx noise floor can be calculated as $P_{nf} = -174 + 10 \log_{10}(800 \times 10^6) + 10 = -75$ dBm.

We consider UE locations at a step size of 1 m on each sidewalk. The median path gain for each BS and UE pair with a link distance of d is obtained based on the path gain equation (4) with slope (n), intercept (b), and RMS (σ) values given by Table 1. The link SNR value at each UE location with link distance of d is computed as

$$\text{SNR}(d) = P_{Tx} + G_{Tx} + \text{PG}_{\text{med}}(d) + G_{Rx} - P_{nf}. \quad (5)$$

Fig. 6 shows the resulting link SNR values for individual sidewalks using color bars, where the link SNR value decreases as link distance increases. The range of the achievable median SNR values

¹⁰The resulting maximum total EIRP of +51 dBm is comparable to that of the 28 GHz phased array antenna modules [11] to be deployed in COSMOS.

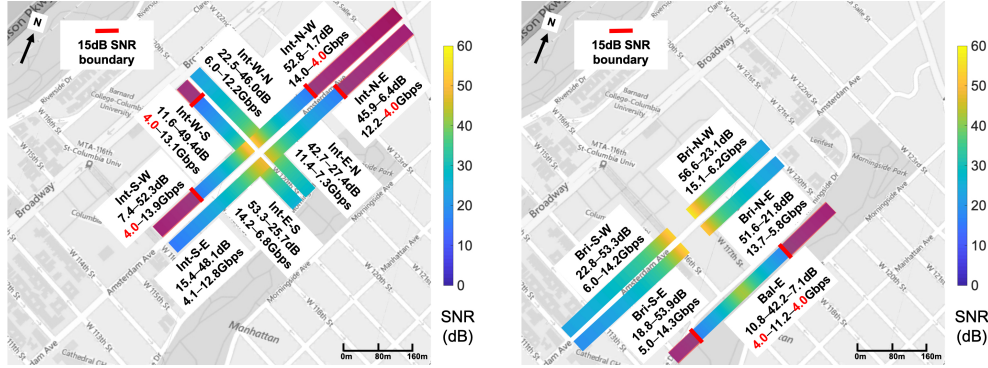


Figure 6: Heatmap of median link SNR values, which are generated using the path gain model (4) with slope (n), intercept (b), and RMS (σ) values given in Table 1, on individual sidewalks in the COSMOS testbed deployment area. The corresponding Shannon rates are also included for individual sidewalks, where UE locations with link SNR values lower than 15 dB are ignored in the rate computation (shaded red area).

is also labeled for each sidewalk, with a cutoff point where the link SNR drops to below 15 dB. In particular, 5 sidewalks have link SNR values lower than 15 dB at the far end, and the smallest cutoff distance is 194 m on Int-S-W. Fig. 6 also shows the corresponding Shannon rates that can be achieved on individual sidewalks, where the UE locations with link SNR values lower than 15 dB are ignored (shaded red area). The results illustrate the theoretically achievable data rates in the considered area.

6 CONCLUSIONS

In this paper, we presented the results of an extensive channel measurement campaign in the COSMOS testbed deployment area. We thoroughly studied 3 sites and obtained measurements of over 1,500 links on 13 sidewalks, some of which were measured multiple times in different settings. We studied the effects of swapped Tx and Rx locations, Tx heights, and seasonal effects on the path gain and concluded that these effects are insignificant in most scenarios. Moreover, we studied the path gain values, the effective azimuth beamforming gain, and median SNR values that can be achieved on the 13 sidewalks. Overall, the results can inform the deployment of the 28 GHz PAAMs in the COSMOS testbed. However, there are several directions for future work, including more extensive studies of seasonal effects in tree-sparse urban street canyons, and wide-band channel measurements for obtaining more detailed channel parameters (e.g., power delay profile) in the same environment.

ACKNOWLEDGMENTS

This work was supported in part by NSF grants ECCS-1547406, CNS-1650685, and CNS-1827923, and Conicyt Project FB 0821. We thank Shiraz Bendor, Shounak Roy, Kimberly Santiago, and Jackson Welles for their help with the measurements.

REFERENCES

- [1] Cloud enhanced Open Software defined MOBILE wireless testbed for city-Scale deployment (COSMOS). <https://cosmos-lab.org/>, 2018.
- [2] Jiakai Yu, Tingjun Chen, Craig Gutterman, Shengxiang Zhu, Gil Zussman, Ivan Seskar, and Dan Kilper. COSMOS: Optical architecture and prototyping. In *Proc. OSA OFC'19*, 2019.
- [3] Theodore S Rappaport, Shu Sun, Rimma Mayzus, Hang Zhao, Yaniv Azar, Kevin Wang, George N Wong, Jocelyn K Schulz, Mathew Samimi, and Felix Gutierrez. Millimeter wave mobile communications for 5G cellular: It will work! *IEEE Access*, 1:335–349, 2013.
- [4] Zhouyue Pi and Farooq Khan. An introduction to millimeter-wave mobile broadband systems. *IEEE Commun. Mag.*, 49(6):101–107, 2011.
- [5] Yasaman Ghasempour, Muhammad K Haider, Carlos Cordeiro, Dimitrios Koutsonikolas, and Edward Knightly. Multi-stream beam-training for mmWave MIMO networks. In *Proc. ACM MobiCom'18*, 2018.
- [6] Joe Chen, Daniel Steinmetzer, Jiska Classen, Edward Knightly, and Matthias Hollick. Pseudo lateration: Millimeter-wave localization using a single RF chain. In *Proc. IEEE WCNC'17*, 2017.
- [7] Omid Abari, Dinesh Bharadia, Austin Duffield, and Dina Katabi. Enabling high-quality untethered virtual reality. In *Proc. USENIX NSDI'17*, 2017.
- [8] Theodore S Rappaport, Felix Gutierrez, Eshar Ben-Dor, James N Murdock, Yijun Qiao, and Jonathan I Tamir. Broadband millimeter-wave propagation measurements and models using adaptive-beam antennas for outdoor urban cellular communications. *IEEE Trans. Antennas Propag.*, 61(4):1850–1859, 2012.
- [9] Theodore S Rappaport, George R MacCartney, Mathew K Samimi, and Shu Sun. Wideband millimeter-wave propagation measurements and channel models for future wireless communication system design. *IEEE Trans. Commun.*, 63(9):3029–3056, 2015.
- [10] Jialiang Zhang, Xinyu Zhang, Pushkar Kulkarni, and Parmesh Ramanathan. OpenMili: a 60 GHz software radio with a programmable phased-array antenna. In *Proc. ACM MobiCom'16*, 2016.
- [11] Bodhisatwa Sadhu, Yahya Touse, Joakim Hallin, Stefan Sahl, Scott K Reynolds, Örjan Renström, Kristoffer Sjögren, Olov Haapalahti, Nadav Mazar, Bo Bokning, et al. A 28 GHz 32-element TRX phased-array IC with concurrent dual-polarized operation and orthogonal phase and gain control for 5G communications. *IEEE J. Solid-State Circuits*, 52(12):3373–3391, 2017.
- [12] Swetank Kumar Saha, Yasaman Ghasempour, Muhammad Kumail Haider, Tariq Siddiqui, Paulo De Melo, Neerad Somanchi, Luke Zakrajsek, Arjun Singh, Roshan Shyamsunder, Owen Torres, et al. X60: A programmable testbed for wideband 60 GHz WLANs with phased arrays. *Computer Communications*, 133, 2019.
- [13] C Umit Bas, Rui Wang, Seun Sangodoyin, Dimitris Psychoudakis, Thomas Henige, Robert Monroe, Jeongho Park, Jianzhong Zhang, and Andreas F Molisch. Real-time millimeter-wave MIMO channel sounder for dynamic directional measurements. *arXiv preprint arXiv:1807.11921*, 2018.
- [14] 5G: Study on channel model for frequencies from 0.5 to 100 GHz (3GPP TR 38.901 version 14.0.0 Release 14). https://www.etsi.org/deliver/etsi_tr/138900/138999/138901/14.00.00_60/tr_138901v140000p.pdf, 2017.
- [15] George R MacCartney, Mathew K Samimi, and Theodore S Rappaport. Omnidirectional path loss models in New York City at 28 GHz and 73 GHz. In *Proc. IEEE PIMRC'14*, 2014.
- [16] Andreas F Molisch, Aki Karttunen, Rui Wang, C Umit Bas, Sooyoung Hur, Jeongho Park, and Jianzhong Zhang. Millimeter-wave channels in urban environments. In *Proc. EuCAP'16*, 2016.
- [17] C Umit Bas, Rui Wang, Seun Sangodoyin, Sooyoung Hur, Kuyeon Whang, Jeongho Park, Jianzhong Zhang, and Andreas F Molisch. 28 GHz microcell measurement campaign for residential environment. In *Proc. IEEE GLOBECOM'17*, 2017.
- [18] Yaguang Zhang, Soumya Jyoti, Christopher R Anderson, David J Love, Nicolo Michelusi, Alex Sprintson, and James V Krogmeier. 28 GHz channel measurements and modeling for suburban environments. In *Proc. IEEE ICC'18*, 2018.
- [19] Sanjib Sur, Vignesh Venkateswaran, Xinyu Zhang, and Parmesh Ramanathan. 60 GHz indoor networking through flexible beams: A link-level profiling. In *Proc. ACM SIGMETRICS'15*, 2015.
- [20] Daniel Steinmetzer, Daniel Wegemer, Matthias Schulz, Joerg Widmer, and Matthias Hollick. Compressive millimeter-wave sector selection in off-the-shelf IEEE 802.11ad devices. In *Proc. ACM CoNEXT'17*, 2017.
- [21] Jinfeng Du, Dmitry Chizhik, Rodolfo Feick, Mauricio Rodriguez, Guillermo Castro, Reinaldo Valenzuela, et al. Suburban fixed wireless access channel measurements and models at 28 GHz for 90% outdoor coverage. *arXiv preprint arXiv:1807.03763*, 2018.